

# A low-temperature route for the synthesis of nanocrystalline LaB<sub>6</sub>

Maofeng Zhang<sup>a</sup>, Liang Yuan<sup>b</sup>, Xiaoqing Wang<sup>a</sup>, Hai Fan<sup>a</sup>, Xuyang Wang<sup>a</sup>,  
Xueying Wu<sup>a</sup>, Haizhen Wang<sup>a</sup>, Yitai Qian<sup>a,\*</sup>

<sup>a</sup>Hefei National Laboratory for Physical Sciences at Microscale, Department of Chemistry, University of Science and Technology of China, Hefei 230026, PR China

<sup>b</sup>Agricultural Department, Shangqiu Vocational and Technical College, Shangqiu 476100, PR China

Received 19 September 2007; received in revised form 19 November 2007; accepted 16 December 2007

Available online 23 December 2007

## Abstract

Nanocrystalline lanthanum hexaboride (LaB<sub>6</sub>) with mean particle size of 30 nm has been successfully synthesized at 400 °C in an autoclave starting from metallic magnesium powder, NaBH<sub>4</sub> and LaCl<sub>3</sub>. In this case, by using B<sub>2</sub>O<sub>3</sub> instead of NaBH<sub>4</sub>, LaB<sub>6</sub> nanocubes with mean size of ~200 nm were formed at 500 °C. The X-ray diffraction (XRD) pattern can be indexed as cubic LaB<sub>6</sub> with the lattice constant of  $a = 4.151 \text{ \AA}$  for LaB<sub>6</sub> nanoparticles and 4.154 Å for LaB<sub>6</sub> nanocubes. An atomic ratio of La and B as 1:5.94 was determined from EDS for LaB<sub>6</sub> nanoparticles. XPS data of LaB<sub>6</sub> nanocubes indicate the atomic ratio of La to B as 1:5.95. Raman spectra indicate the formation of LaB<sub>6</sub>. © 2008 Elsevier Inc. All rights reserved.

**Keywords:** LaB<sub>6</sub>; Nanoparticles; Nanocubes; Low temperature; Synthesis

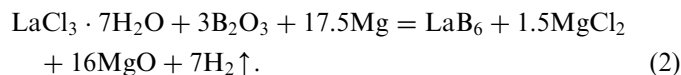
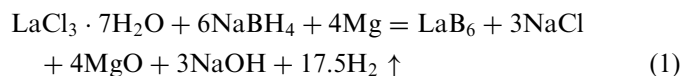
## 1. Introduction

Lanthanum hexaboride (LaB<sub>6</sub>) is a refractory compound characterized by a high melting temperature, excellent thermal stability, high hardness, and has found application as one of the most widely used thermionic electron sources in a large variety of devices requiring electron emission which can offer high brightness and long service life, because of its low work function (~2.6 eV) [1,2], high current and voltage capability, and low vapor pressure at high temperature [3].

Usually, LaB<sub>6</sub> is prepared by high-temperature reaction, such as the direct solid-phase reaction of lanthanum or its oxides with elemental boron around 1800 °C [4–7], the floating zone method of rare-earth oxides with boron at 1700 °C [8], carbothermal reduction of lanthanum oxide and boron at 1500 °C [9], the aluminum flux using LaCl<sub>3</sub> and B<sub>2</sub>O<sub>3</sub> as precursors around 1500 °C [10], chemical vapor deposition (CVD) method using LaCl<sub>3</sub> powders and BCl<sub>3</sub> gas in an atmosphere of hydrogen and nitrogen at 1150 °C [11,12]. Recently, LaB<sub>6</sub> crystals have been synthe-

sized from molten salt electrolysis at 850 °C [13]. Also, LaB<sub>6</sub> thin films were deposited by the pulsed laser deposition (PLD) technique at 850 °C [2].

In this paper, we report a convenient route to prepare LaB<sub>6</sub> nanoparticles at 400 °C via a solid-state reaction of metallic magnesium powder with NaBH<sub>4</sub> and LaCl<sub>3</sub> in an autoclave. In this case, LaB<sub>6</sub> nanocubes were prepared at 500 °C by using B<sub>2</sub>O<sub>3</sub> instead of NaBH<sub>4</sub>. The reactions can be described as follows:



## 2. Experimental

### 2.1. Sample preparation

#### 2.1.1. Preparation of LaB<sub>6</sub> nanoparticles

In a typical procedure, appropriate amounts of LaCl<sub>3</sub>·7H<sub>2</sub>O (1.114 g), excessive NaBH<sub>4</sub> (1.000 g), and excessive

\*Corresponding author.

E-mail address: [ytqian@ustc.edu.cn](mailto:ytqian@ustc.edu.cn) (Y. Qian).

Mg (0.800 g) were put into a stainless steel autoclave of 25 ml capacity. Then, the autoclave was sealed under Ar atmosphere and maintained at 400 °C for 4 h, followed by naturally cooling to room temperature. The products were washed with distilled water and dilute hydrochloric acid, respectively, to remove Na, NaCl, MgO and other impurities. The final products were vacuum-dried at 60 °C for 4 h. Purple powders were obtained.

### 2.1.2. Preparation of LaB<sub>6</sub> nanocubes

In a typical procedure, appropriate amounts of LaCl<sub>3</sub>·7H<sub>2</sub>O (0.003 mol), B<sub>2</sub>O<sub>3</sub> (0.009 mol), and excessive Mg (0.075 mol) were put into a stainless steel autoclave of 25 ml capacity. Then, the autoclave was sealed under Ar atmosphere and maintained at 500 °C for 4 h, followed by naturally cooling to room temperature. The product was washed with dilute hydrochloric acid and distilled water, respectively, to remove MgO, MgCl<sub>2</sub> and other impurities. The final products were vacuum-dried at 60 °C for 4 h. Purple powders were obtained.

### 2.2. Sample characterization

The phase and composition of the products were determined by a Rigaku D/Max-γA rotating-anode X-ray diffractometer equipped with monochromatic high-intensity CuKα radiation ( $\lambda = 1.54178 \text{ \AA}$ ). X-ray photoelectron spectra (XPS) were recorded on a VG ESCALAB MKII X-ray photoelectron spectrometer using non-monochromatized MgKα X-rays as the excitation source. The morphologies of the samples were observed with a transmission electron microscope (TEM; JEOL-2010) with an attached EDS (energy-dispersive X-ray spectrum) system having an accelerating voltage of 200 kV with a tungsten filament. FESEM images were taken on a JEOL JSM-6300F SEM. Raman spectra were measured on a LABRAM-HR Raman spectrophotometer. The 514.5-nm laser was used as an excitation light source.

### 3. Results and discussion

The lattice parameters and the phase purity of the materials were determined by X-ray diffraction (XRD). Typical XRD patterns of the as-prepared LaB<sub>6</sub> nanoparticles and nanocubes are presented in Figs. 1 and 2, respectively. All the reflection peaks of the products can be easily indexed as cubic crystal system (space group: *pm3m* (221)) of LaB<sub>6</sub> with a calculated lattice constant  $a = 4.151 \pm 0.001 \text{ \AA}$  for LaB<sub>6</sub> nanoparticles and  $4.154 \pm 0.001 \text{ \AA}$  for LaB<sub>6</sub> nanocubes, which is in good agreement with the literature value of  $a = 4.153 \text{ \AA}$  and 4.156 (JCPDS Card No: 06-0401, 34-0427). No other impurity peaks were detected.

EDS analysis of LaB<sub>6</sub> nanoparticles, shown in Fig. 3, reveals the presence of La and B with an atomic ratio of  $1:5.94 \pm 0.03$ . Fig. 4 gives the XPS spectra of the as-prepared LaB<sub>6</sub> nanocubes. The B 1s and La 3d core-level

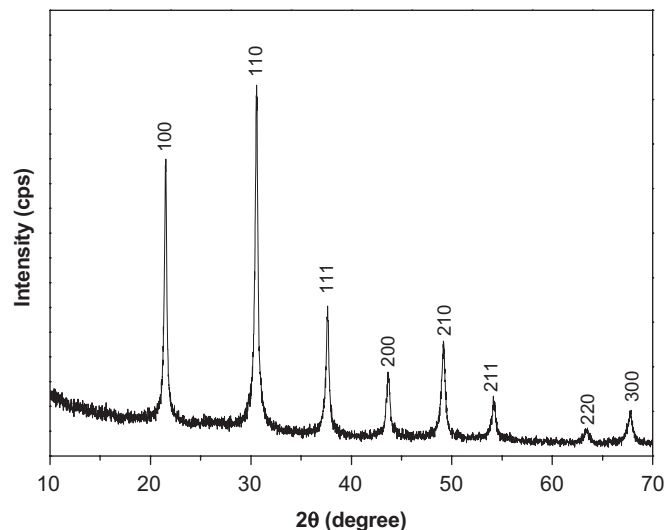


Fig. 1. XRD pattern of the LaB<sub>6</sub> nanoparticles.

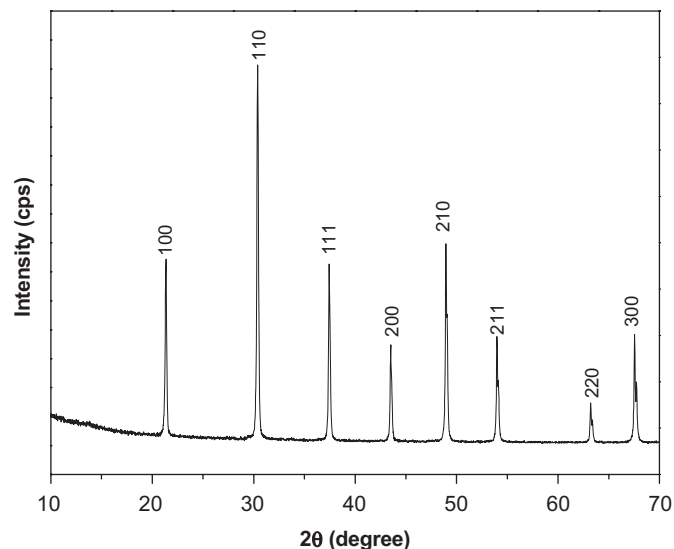


Fig. 2. XRD pattern of the LaB<sub>6</sub> nanocubes.

regions were examined. The binding energy of B 1s is found at 186.7 eV and that of La 3d at 836.8 and 853.1 eV. This corresponds well with the reported binding energies for LaB<sub>6</sub>, confirming the formation of LaB<sub>6</sub>. Based on the calculation of the peak areas, the mole ratio of La/B was obtained to be  $1:5.95 \pm 0.02$ , which is close to the chemical stoichiometry of LaB<sub>6</sub>. Small amounts of nitrogen, oxygen and carbon were also detected from the XPS spectra, which may be due to the absorption of nitrogen, oxygen and carbon on the powder surface.

Fig. 5a shows the TEM image of the LaB<sub>6</sub> nanoparticles. It can be seen that LaB<sub>6</sub> crystallites are nanoparticles with mean grain size of  $\sim 30 \text{ nm}$ , which corresponds to the calculated average result from the Scherrer equation. Fig. 5b shows the SAED pattern of LaB<sub>6</sub>, which is consistent with the high crystallinity of the sample and reveals three clear diffraction rings in accordance with the

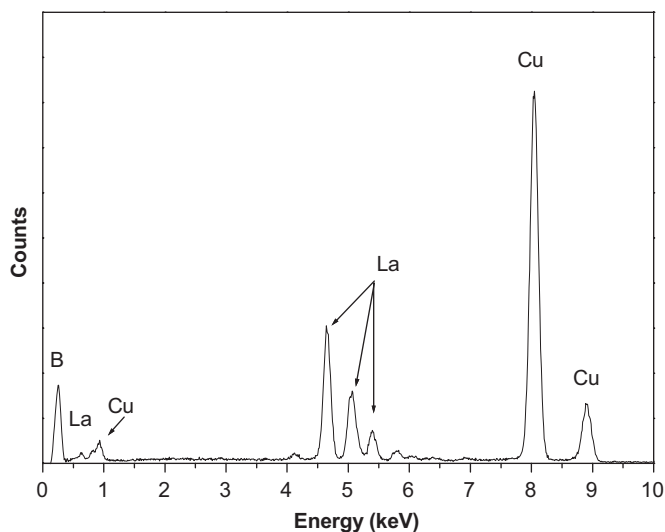


Fig. 3. EDS analysis of the  $\text{LaB}_6$  nanoparticles, showing the presence of La and B.

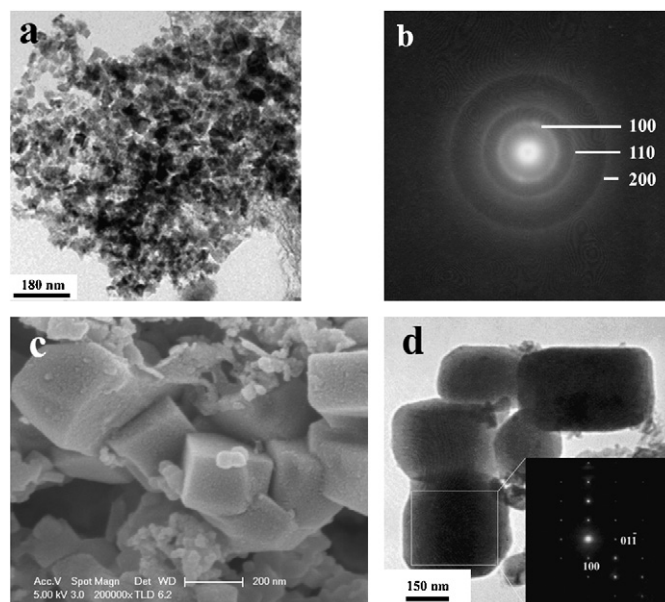


Fig. 5. (a) TEM image and (b) SAED pattern of the  $\text{LaB}_6$  nanoparticles, (c) FESEM image of the  $\text{LaB}_6$  nanocubes and (d) TEM image and SAED pattern of the  $\text{LaB}_6$  nanocubes.

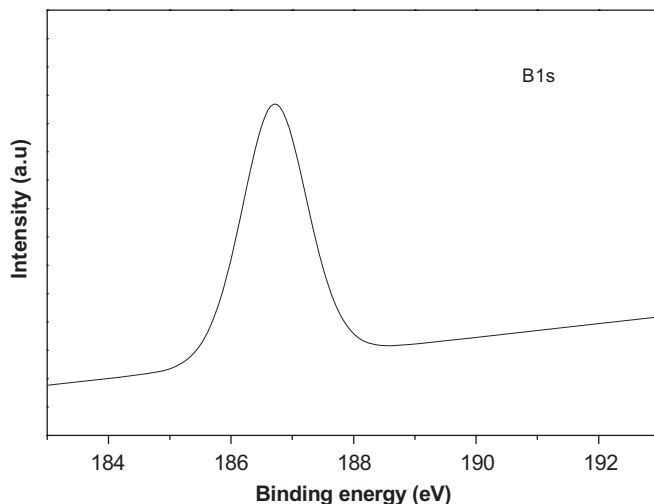
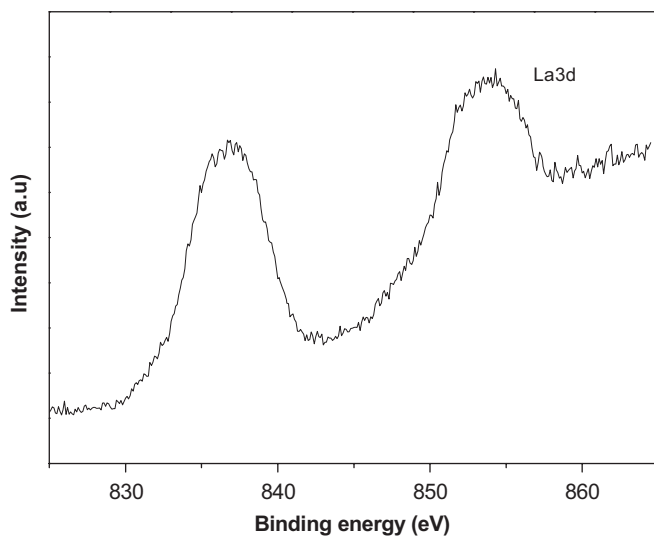


Fig. 4. XPS spectra of the  $\text{LaB}_6$  nanocubes.

(100), (110), (200) crystal planes of cubic  $\text{LaB}_6$ . Fig. 5c shows FESEM image of the  $\text{LaB}_6$  nanocubes. As can be seen,  $\text{LaB}_6$  crystallites are nanocubes with average particle size of  $\sim 200$  nm, which corresponds to the calculated average result from the Scherrer equation. A low-magnification TEM image and SAED pattern of the  $\text{LaB}_6$  nanocubes are shown in Fig. 5d. The SAED pattern of the edge of the selected area taken along the  $\langle 011 \rangle$  zone axis indicates the single-crystalline nature of individual  $\text{LaB}_6$  nanocube.

Figs. 6 and 7 show the Raman spectra of the  $\text{LaB}_6$  nanoparticles and nanocubes at room temperature. The three expected main peaks were observed around 680 ( $T_{2g}$ ), 1120 ( $E_g$ ) and 1250 ( $A_{1g}$ )  $\text{cm}^{-1}$ , which are in agreement with earlier reports [14–16], and they completely satisfy the polarization selection rule in the cubic symmetry. Other two bands around 200 and 1130  $\text{cm}^{-1}$  are characteristic of  $\text{LaB}_6$  sample, as observed in the literature [17]. A broad peak around 1400  $\text{cm}^{-1}$ , labeled as “■”, is commonly observed with a relatively strong intensity for trivalent and intermediate-valent crystals [18]. The above Raman spectra both indicate the formation of  $\text{LaB}_6$ .

In the present preparation process, it is found that the reaction temperature and time play important roles in the formation of  $\text{LaB}_6$ . For  $\text{LaB}_6$  nanoparticles, no  $\text{LaB}_6$  could be obtained if the temperature is below 350 °C. An optimum reaction temperature for  $\text{LaB}_6$  is about 400 °C. And for  $\text{LaB}_6$  nanocubes, the optimum reaction temperature is about 500 °C. No  $\text{LaB}_6$  could be prepared if the temperature is below 400 °C. A series of detailed temperature-dependent experiments reveal that further increase of the reaction temperature over their optimum reaction temperature resulted in an increase of the particle size.

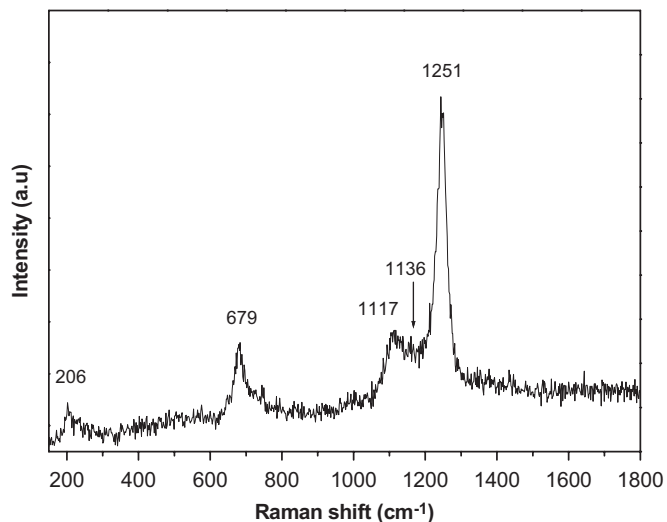


Fig. 6. Raman spectra of the LaB<sub>6</sub> nanoparticles at room temperature.

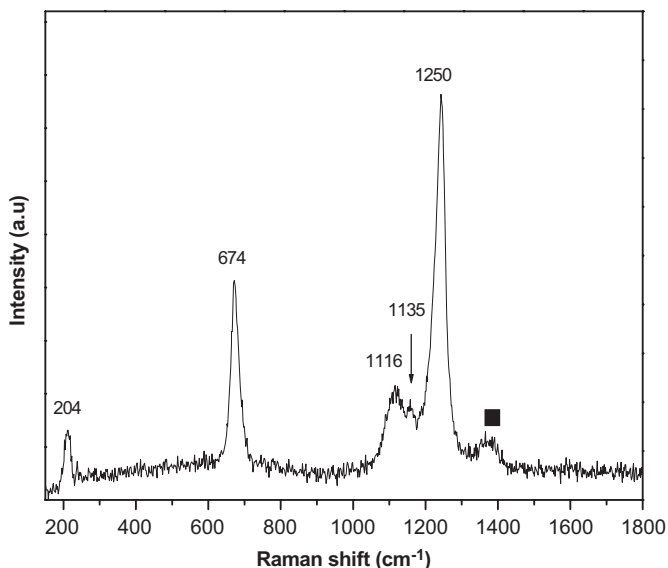


Fig. 7. Raman spectra of the LaB<sub>6</sub> nanocubes at room temperature.

Varying the reaction time between 4 and 12 h did not significantly affect the crystallinity or morphology for two kinds of nanocrystalline LaB<sub>6</sub>. If the time was shorter than 2 h, the reaction became very incomplete and the crystallinity was very poor due to too short reaction time. It is noteworthy that one feature of this synthesis route is the high pressure in the autoclave, due to the H<sub>2</sub> (about 110 atm in reaction Eq. (1) and 55 atm in reaction Eq. (2) estimated by the ideal gas law) produced. The high pressure makes the crystalline LaB<sub>6</sub> form at a relatively low temperature.

#### 4. Conclusions

In summary, nanocrystalline LaB<sub>6</sub> with mean particle size of 30 nm has been successfully synthesized at 400 °C in an autoclave starting from metallic magnesium powder, NaBH<sub>4</sub> and LaCl<sub>3</sub>. In this case, by using B<sub>2</sub>O<sub>3</sub> instead of NaBH<sub>4</sub>, LaB<sub>6</sub> nanocubes with mean size of ~200 nm were formed at 500 °C. XRD pattern and Raman spectra both indicate the formation of LaB<sub>6</sub>. An atomic ratio of B to La close to 6:1 was determined from EDS and XPS. In comparison with previous routes, the present route allows for the formation of nanocrystalline LaB<sub>6</sub> through a simpler process and at a much lower synthesis temperature. This method may be extended to synthesize other rare-earth metal borides.

#### Acknowledgments

This work was supported by the National Natural Science Foundation of China (No. 20431020) and the 973 Project of China (No. 2005CB623601).

#### References

- [1] M. Gesley, L.W. Swanson, *Surf. Sci.* 146 (1984) 583–599.
- [2] V. Craciun, D. Craciun, *Appl. Surf. Sci.* 247 (2005) 384–389.
- [3] L.W. Swanson, M.A. Gesley, P.R. Davis, *Surf. Sci.* 107 (1981) 263–289.
- [4] J.M. Lafferty, *J. Appl. Phys.* 22 (1951) 299–309.
- [5] J.R. Rea, E. Kostiner, *J. Crystal Growth* 11 (1971) 110–116.
- [6] B.J. Curtis, H. Graffenberger, *Mater. Res. Bull.* 1 (1966) 27–32.
- [7] T. Niemyski, I. Procka, J. Jun, J. Paderno, *J. Less Common Met.* 15 (1968) 97–101.
- [8] S. Otani, H. Nakagawa, Y. Nishi, N. Kieda, *J. Solid State Chem.* 154 (2000) 238–241.
- [9] B. Post, D. Moskowitz, F.W. Glaser, *J. Am. Chem. Soc.* 78 (1956) 1800–1802.
- [10] P. Peshev, *J. Solid State Chem.* 133 (1997) 237–242.
- [11] H. Zhang, Q. Zhang, J. Tang, L.C. Qin, *J. Am. Chem. Soc.* 127 (2005) 2862–2863.
- [12] H. Zhang, J. Tang, Q. Zhang, G. Zhao, G. Yang, J. Zhang, O. Zhou, L.C. Qin, *Adv. Mater.* 18 (2006) 87–91.
- [13] M. Kamaludeen, I. Selvaraj, A. Visuvasama, R. Jayavel, *J. Mater. Chem.* 8 (1998) 2205–2207.
- [14] P. Teredesai, D.V.S. Muthu, N. Chandrabhas, S. Meenakshi, V. Vijayakumar, P. Modak, R.S. Rao, B.K. Godwal, S.K. Sikka, A.K. Sood, *Solid State Commun.* 129 (2004) 791–796.
- [15] Z. Yahia, S. Turrell, G. Turrell, J.P. Mercurio, *J. Mol. Struct.* 224 (1990) 303–306.
- [16] Z. Yahia, S. Turrell, J.P. Mercurio, G. Turrell, *J. Raman Spectrosc.* 24 (1993) 207–212.
- [17] R. Schmechel, H. Werheit, Y.B. Paderno, *J. Solid State Chem.* 133 (1997) 234–268.
- [18] N. Ogita, S. Nagai, N. Okamoto, M. Udagawa, J. Akimitsu, S. Kunii, *Phys. Rev. B* 68 (2003) 224305–224312.